

## Fission timescale from dynamical model calculation

Charmi Vadagama<sup>1</sup>, M. T. Senthil Kannan<sup>2,3</sup>,  
 Jhilam Sadhukhan<sup>2,3</sup>, and Pruthul Desai<sup>1</sup>

<sup>1</sup>*Department of Physics, Sir P. T. Sarvajanic College of Science, Surat-395007, INDIA*

<sup>2</sup>*Physics Group, Variable Energy Cyclotron Centre,  
 1/AF, Bidhannagar, Kolkata -700064, INDIA and*

<sup>3</sup>*Homi Bhabha National Institute, Anushakti Nagar, Mumbai-400094, INDIA*

### Introduction

The study of fission dynamics is the a challenging subject due to the intricate nature of this process. A compound nucleus (CN) may undergo fission depending on the excitation energy, angular momentum, fission barrier, and other factors. However, the dynamics of the fission process depends principally on the target-projectile combination, viz-*a-viz* the total mass, and the excitation energy. This relevance can be examined by using the fission timescale ( $\tau_f$ ), which is the time required for the CN to reach the scission configuration from the ground state shape. Significant effort has been made to comprehend fission timescales through various experimental techniques. Fission timescales can be inferred from the measured pre-scission multiplicities [1–3], evaporation residue (ER) cross-section and fission probabilities [4, 5]. These nuclear techniques, with a proper model, are used to evaluate the fission time in the range of  $10zs$  ( $1zs = 10^{-21}s$ ). On the other hand, direct probes like the crystal blocking technique and K X-ray measurements determine a much longer lifetime of the order of  $\sim 10^{-18}s$ (*attosecond*). A state-of-the-art one dimensional Langevin dynamical model has been used recently to resolve this discrepancy [7]. In this work, similar study is extended for a wide range of masses with different excitation energies.

### Calculations

A stochastic one-dimensional Langevin approach is utilised to study the full dynamical evolution of an excited compound system. The details of the model can be found in Ref. [6, 7]. In this work, reduced friction pa-

TABLE I: Details of the reactions:

CN	$E^*$ (MeV)	$\nu_{pre}$ (Exp.)	$\nu_{pre}$ (Cal.)	$\beta$ (MeV/ $\hbar$ )	Ref.
<sup>125</sup> Cs	241.78	4.0±0.5	4.0676	4	[1]
<sup>203</sup> At	72.5	2.54±0.23	2.5989	5	[2]
<sup>243</sup> Am	54.1	1.35±0.14	1.4312	0.5	[3]

rameter ( $\beta$ ) is considered as a free parameter to match the experimental neutron multiplicities. A large number of Langevin trajectories  $10^6$  are sampled to reduce the statistical uncertainties. For each event, dynamics is followed numerically up to  $10^{-15}s$  with a time-step of  $10^{-25}s$ . At each time step, evaporation of light particle ( $n$ ,  $p$ ,  $\alpha$ ) and GDR  $\gamma$ -ray are sampled with the Monte-Carlo technique. The standard statistical model prescription is considered to calculate the widths for these evaporation channels. The initial collective coordinate is that of a spherical nucleus, and its initial momentum distribution follows from an equilibrated thermal system. A Langevin trajectory is judged as a fission event when it reaches the scission configuration:  $c_s = 0.3 R_0$  ( $R_0$  being the spherical nucleus radius). For each fission event, fission time is evaluated with associated neutron evaporation fission channels.

### Results and Discussion

The details of the reaction channels, chosen for the present work, are given in the table I.  $\beta$  values are adjusted for each reaction to reproduce the experimental pre-scission neutron multiplicity. Simultaneously, fission yields associated with the different fission channels are calculated. In Fig. 1, the total fission yields of

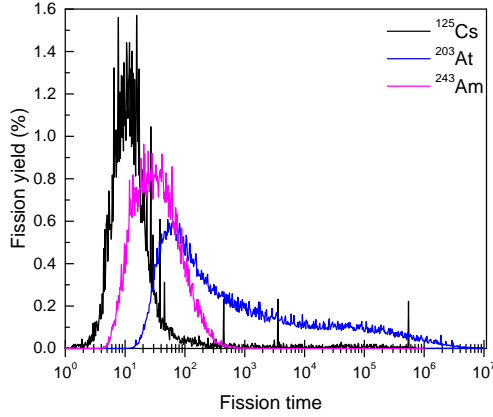


FIG. 1: Fission yield distribution as a function of time for  $^{125}\text{Cs}$ ,  $^{203}\text{At}$  and  $^{243}\text{Am}$

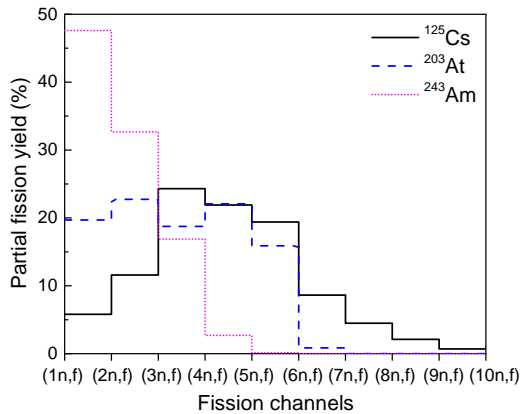


FIG. 2: Partial fission yields from different isotopes of  $^{125}\text{Cs}$ ,  $^{203}\text{At}$  and  $^{243}\text{Am}$  through neutron evaporation.

$^{125}\text{Cs}$ ,  $^{203}\text{At}$ , and  $^{243}\text{Am}$  are shown as a function of fission time. The fission time distribution has a peak around  $10^{-20}\text{s}$  with a very small non-vanishing tail up to  $10^6\text{zs}$  for the  $^{125}\text{Cs}$  compound system. Further, the  $\tau_f$  (scission time) distribution for  $^{203}\text{At}$  has a broader width with a peak around  $10^{-19}\text{s}$ , and has a considerably longer tail up to the maximum dynamical time. Conversely, the actinide nucleus shows a narrower peak with a shorter

fission lifetime  $\sim 10^{-20}\text{s}$ .

From these distributions, we have observed the average fission time ( $\langle\tau_f\rangle$ ),  $2.26 \times 10^{-18}\text{s}$ ,  $4.39 \times 10^{-17}\text{s}$  and  $3.42 \times 10^{-20}\text{s}$  for the systems  $^{125}\text{Cs}$ ,  $^{203}\text{At}$  and  $^{243}\text{Am}$ , respectively. The  $as$  fission timescales for  $\langle\tau_f\rangle$  are mainly contributed by the long tail part of fission yields. Further, to understand the behavior of  $\langle\tau_f\rangle$  in a more clear way, partial fission yields of different fission channels are depicted in Fig. 2. For  $^{125}\text{Cs}$ , fission channels up to  $(8n, f)$  have contributed, which indicate that the CN has survived for longer dynamical time after the last particle evaporated. Because each neutron usually reduces the CN excitation by  $8 - 10$  MeV (separation energy + kinetic energy), it makes the fission process slower. The same scenario is valid for  $^{203}\text{At}$  up to  $(6n, f)$  fission channel. For this system, available  $E^*$  falls between  $15 - 25$  MeV, hence the substantial percentage of CN persists for a longer time. In contrast, larger partial fission yield is observed for the  $(1n, f)$  and  $(2n, f)$  channels for  $^{243}\text{Am}$ , resulting a very short fission timescale. From this study, we conclude that the fission timescale primarily depends on the mass of the CN, which determines the potential energy surface (PES). Consequently, the fission timescale of each nucleus is determined by the shape of PES near the ground state configuration.

## References

- [1] Hinde *et al.*, *Phy. Rev. C* **45**, 1229 (1992).
- [2] K. Ramchandran *et al.*, *Phys. Rev. C* **73**, 064609 (2006).
- [3] Saxena *et al.*, *Phy. Rev. C* **49**, 932 (1994).
- [4] B. B. Back *et al.*, *Phys. Rev. C* **60**, 044602 (1999).
- [5] B. Lott *et al.*, *Phys. Rev. C* **63**, 034616 (2001).
- [6] J. Sadhukhan and S. Pal, *Phys. Rev. C* **79**, 064606 (2009).
- [7] M. T. Senthil Kanan *et al.*, *Phys. Rev. C* **98**, 021601 (2018).